THE JOHNS HOPKINS UNIVERSITY
APPLIED PHYSICS LABORATORY
8621 Georgia Avenue, Silver Spring, Maryland

CM-1026

Operating under Contract NOw 62-0604-c with the
Bureau of Naval Weapons, Department of the Navy

Copy No. 19

BIOSATELLITE RECOVERY FROM CIRCULAR ORBITS

by

C. J. Swet

October 1962

CM-1026
October 1962

Biosatellite Recovery from Circular Orbits

by

C. J. Swet

THE JOHNS HOPKINS UNIVERSITY
APPLIED PHYSICS LABORATORY
8621 GEORGIA AVENUE SILVER SPRING, MARYLAND

The Johns Hopkins University
APPLIED PHYSICS LABORATORY
Silver Spring, Maryland

ABSTRACT

This report is a primer for the non-ballistician who is concerned with the design or selection of biospace experiments, to provide him with some feeling for the ballistics of biosatellite recovery. It presents in non-specialized terms some results of a recent parametric study of a wide variety of likely descent trajectories from near-earth orbits. Although these results were computed by approximate methods, they are believed to be sufficiently accurate for most planning purposes. No attempt is made to describe the computational methods or the underlying physics.

TABLE OF CONTENTS

LIST OF ILLUSTRATIONS

LIST OF TABLES

The Johns Hopkins University
APPLIED PHYSICS LABORATORY
Silver Spring, Maryland

BIOSATELLITE RECOVERY FROM CIRCULAR ORBITS

I. INTRODUCTION

Biosatellite recovery involves a gamut of situations midway between those encountered by long range bombardment missiles and manned spacecraft and shares many problems of each genre which are not common to both. Cost and other practical considerations favor the steep unguided descent trajectory of a ballistic missile, while equally compelling factors such as available mass fraction and payload g-tolerance promote the shallower entries typical of manned orbital missions.

Although the literature abounds with excellent analytical treatments of the descent and re-entry regimes, few are in evidence which cover this middle ground of particular interest to the biospace scientist. Even less abundant are those which discuss both regimes as the continuum that they actually represent, in terms which are meaningful to the non-specialist.

This paper is intended to fill partially the persisting need for a non-rigorous, yet factually illuminating and useful presentation of those parameters which are of vital interest to the planners of biospace experiments.

II. DISCUSSION

Interest here is confined to the fairly straightforward (and probably the most prevalent) case of ballistic re-entry from a deflected circular orbit. This implies a non-lifting capsule geometry such as that of Mercury or Discoverer with no maneuvers in the atmosphere other than parachute deployment during the terminal phase of re-entry. It also means that the original orbit is deflected into a descent trajectory by one brief firing of a retro-rocket, as illustrated in Fig. 1. By looking only at circular orbits, complicated presentations are avoided without seriously departing from practical reality since a circular model applies fairly closely at the slight eccentricities (up to about 100 miles difference between apogee and perigee) which normally result from launch dispersions. Also, this approach is applicable whenever a highly eccentric orbit must be circularized as an intermediate step toward recovery. The problem of direct descent from substantially eccentric orbits will be considered in another paper.

Nine trajectory parameters (seven of which are indicated in Fig. 2) will be examined. The three which define initial conditions which essentially determine the other six features of the subsequent path to impact are:

1. Circular altitude of the original orbit,
2. Magnitude of the deflecting velocity change, and
3. Direction of the deflecting velocity change.

Another three represent usual trajectory constraints imposed by biological and other considerations, with which the choice of initial conditions must be reconciled.

4. Peak deceleration during re-entry,
5. Total range to impact, and
6. Range error, (a) due to aiming errors, and
   (b) due to retro-rocket impulse dispersion.

The remaining three relate to the atmospheric entry point, where a descending vehicle theoretically leaves the domain of celestial mechanics and enters that of aerodynamics. These are of less compelling interest to the mission planner because they describe an intermediate situation which is not limiting per se, but are included here to highlight trends and to facilitate more detailed analysis of the re-entry phase. They are:

7. Range to entry,
8. Entry angle, and
9. Entry velocity.

Only the downrange (in the orbital plane) components of these parameters are considered here, since the cross-range (normal to the orbital plane) components are generally orders of magnitude smaller. Re-entry heating is ignored because it is a condition that can be mitigated by vehicle design, whereas all of the other characteristics are virtually unalterable consequences of the initial conditions. It has been assumed that the earth and its atmosphere is non-rotating, which makes this presentation apply to orbits of any inclination without appreciably degrading its validity. All of the indicated relationships are totally independent of vehicle weight, and vary only slightly over the entire range of likely re-entry geometries.

Interest in peak deceleration extends to a value of about 50g, which appears to be the maximum that could conceivably be endured by a small primate for more than a few seconds. As an upper limit for the magnitude of the deflecting velocity change, 4000 ft/sec has been somewhat arbitrarily selected which, as shown in Fig. 3, would require a retro-rocket weighing roughly half as much as the vehicle it de-orbits. For missions requiring impact prediction to accuracies of 50 miles or better, these bounds automatically place an altitude limit of about 800 n. miles on the circular orbits from which a single-impulse descent can be reasonably considered.

Figure 4 illustrates how range and range errors are affected by both the magnitude and direction of the deflecting velocity change for a given orbit of 300 n. miles altitude. Note that for each magnitude of the velocity change a different thrust orientation angle yields minimum total range to impact, at which condition impact accuracy is scarcely affected by small angular errors. The degree of sensitivity to this source of error is indicated by the flatness of each curve at its null point, with the larger retro-rockets producing the flatter curves (higher accuracy). At the null point for the 1000 ft/sec curve, an angular error of 5° contributes less than 0.5° (30 n. miles) to the range error. For 4000 ft/sec a tolerance of over 10° could assure the same accuracy. The distance traveled in the atmosphere (the difference between corresponding curves for range to entry and range to impact) varies in a like manner, showing that the larger retro-rocket will also shorten the re-entry portion of descent, and reduce the impact dispersions created by unpredictable variations in the troposphere.

Figure 5 presents the atmospheric entry angle as a function of the same parameters for the same orbital altitude. As would be expected, comparison with Fig. 4 shows that the steeper angles correspond to shorter re-entry regimes and equivalently higher accuracy.

In the same fashion, Fig. 6 presents the velocity at atmospheric entry. As might also be expected, a vehicle enters the atmosphere more slowly when more braking impulse is provided by the retro-rocket.

In Fig. 7 the effects may be seen of these variable initial conditions on the peak deceleration which occurs during atmospheric penetration. Note that when the retro-rocket is aimed for minimum range, gross aiming errors produce quite modest variations in g-loading. It should also be recognized that, although the magnitude of peak deceleration is virtually independent of the re-entry vehicle shape, its onset rate, and the altitude and velocity at which it occurs, are significantly affected by the weight-to-drag ratio.

For the same example Fig. 8 shows how variations in rocket impulse affect impact accuracy. Note particularly that this contribution to range error is expressed as a percentage of the deflecting velocity change, in order to reflect most meaningfully the variations in rocket impulse which cause it. Present state of the art for solid propellant rockets can reasonably assure a scatter of less than 2 per cent about the nominal total impulse. These curves clearly indicate that this source of error cannot be materially reduced by changing the thrust orientation to an angle other than that which yields minimum range. In fact, the resulting increase in sensitivity to angular

errors (referring back to Fig. 4) would generally more than offset any slight gains.

From the foregoing it is fairly evident that the shortest route to impact is usually the optimal route. Accepting this somewhat over-simplified premise makes our problem of data presentation much more tractable.

Figure 9 presents the thrust orientation angles which produce minimum range (which might be construed as optimal) for the entire range of altitudes and deflecting velocities. Since these data represent null points in curves of varying flatness, their importance varies accordingly. A feeling for this can be obtained from Figs. 16 through 22, which present the parameters of Fig. 4 at other altitudes.

Figure 10 similarly presents all data for minimum total range to impact. To provide additional perspective, Fig. 11 describes pictorially how this information might apply to a specific mission: in this case recovery at White Sands from a polar orbit.

The over-all trends in atmospheric entry conditions are illustrated in Figs. 12 and 13. Of particular value are the curves for entry angle, which indicate the length of residence in the atmosphere with its attendant impact errors.

Figure 14 summarizes our findings on peak deceleration, while Fig. 15 collects all of the data on velocity — caused impact errors for minimum range descent trajectories. It is apparent from Fig. 15 that the higher the altitude (and from Fig. 12, the steeper the entry angle) the larger will be the proportion of impact error from this source.

Tables I through VIII present in tabular form the computer output data from which the curves were derived.

Other tentative inferences can and should be drawn from the material which has been presented here, but the reader is cautioned against using any of them out of context. In no event should these data be used as the sole basis for system selection, regardless of accuracy requirements, since a variety of qualifying considerations which are not dealt with here may prove to be of overriding importance.

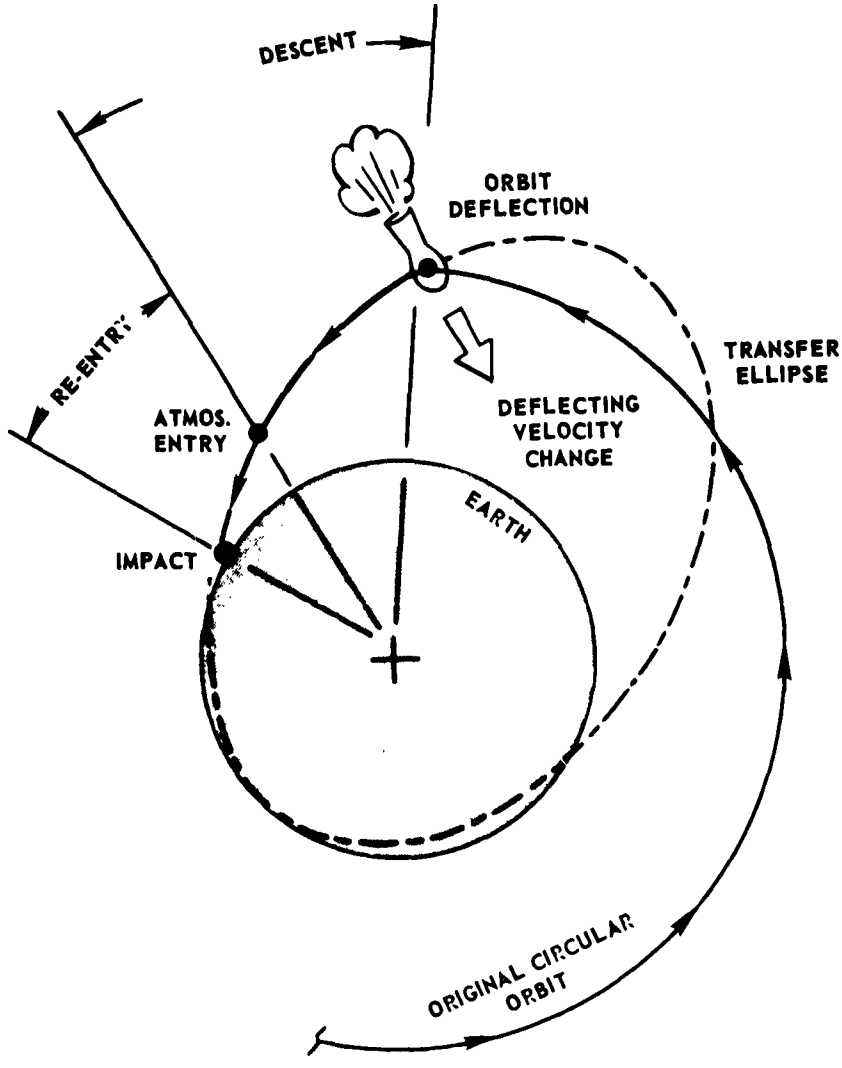

Fig. 1 ONE-IMPULSE DESCENT FROM A CIRCULAR ORBIT

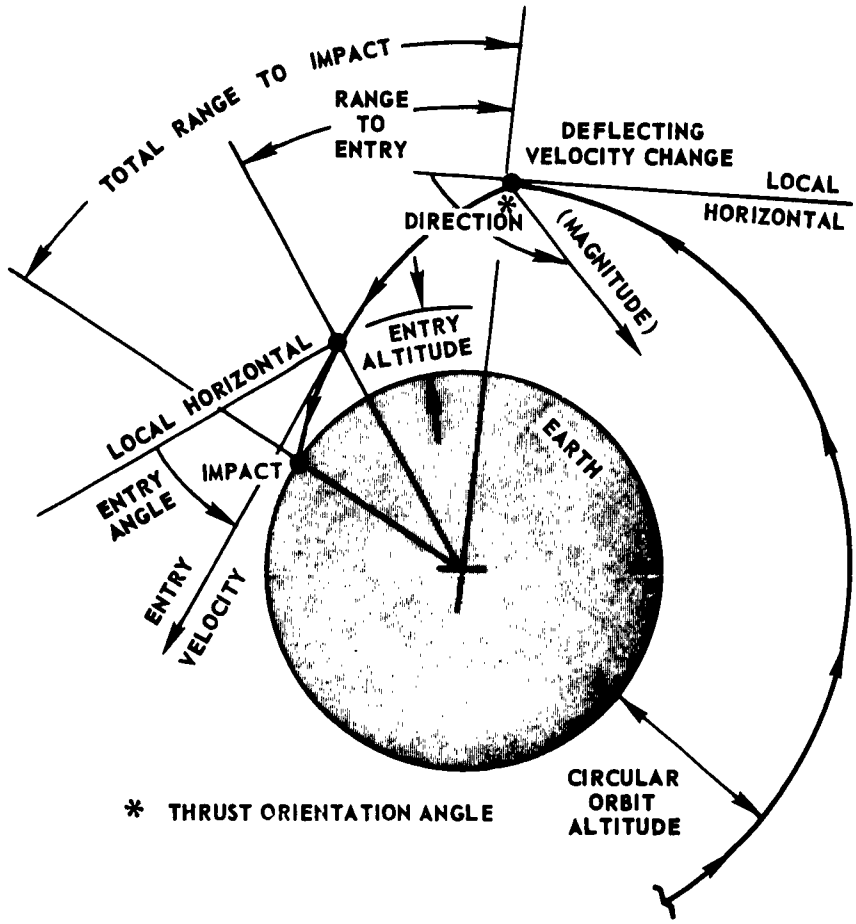

Fig. 2 PARAMETERS OF INTEREST

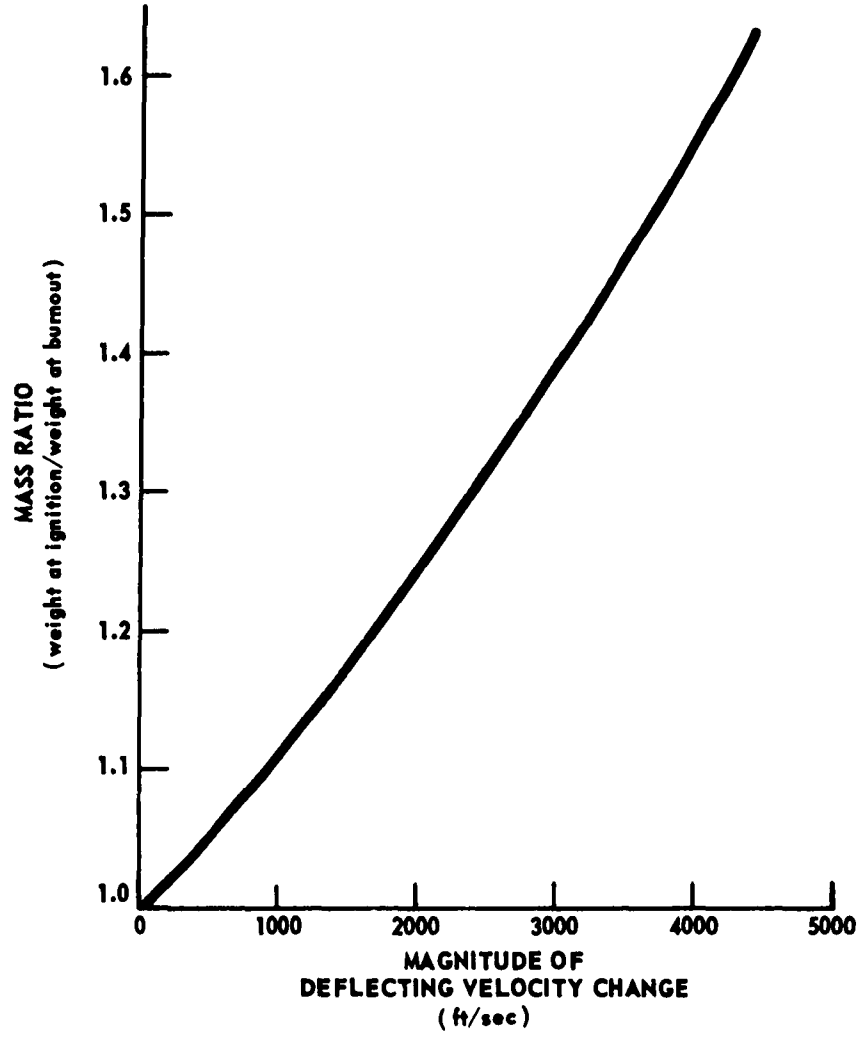

Fig. 3 MASS RATIO VERSUS MAGNITUDE OF DEFLECTING VELOCITY CHANGE
($I_{sp(vac)}$ = 280)

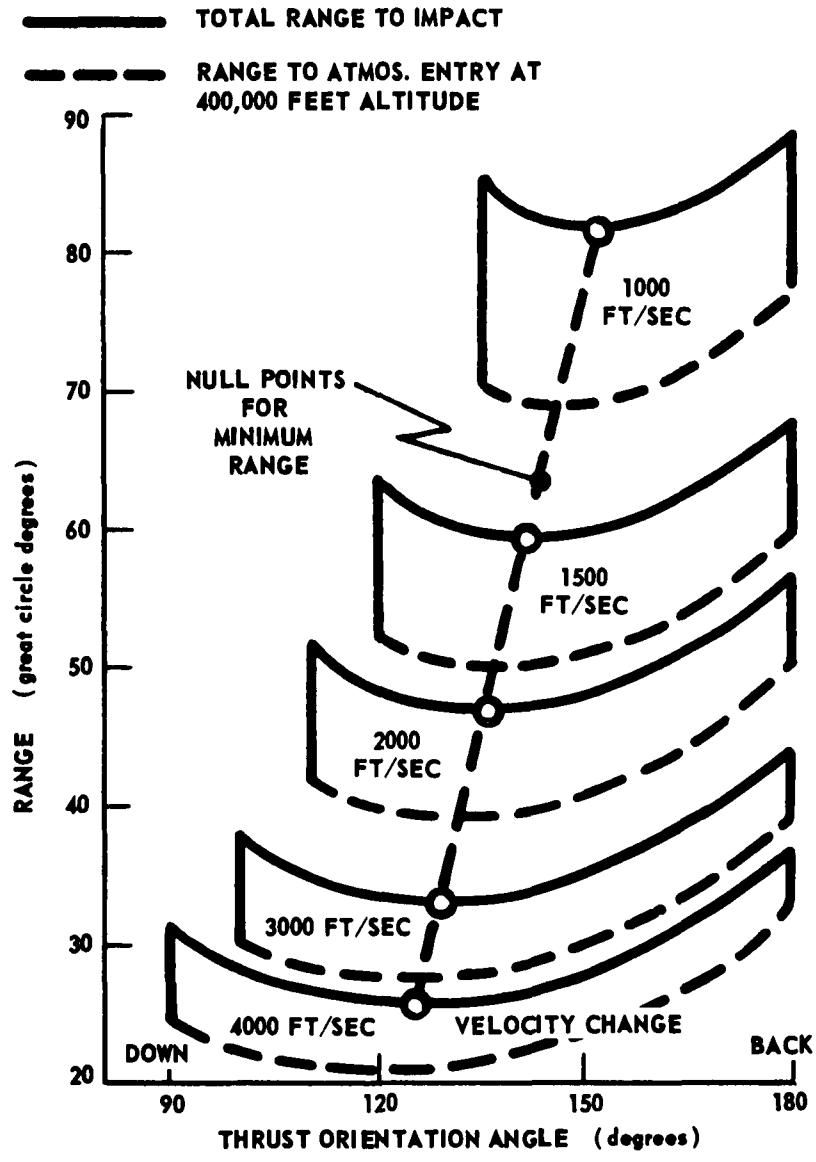

Fig. 4 RANGE VERSUS MAGNITUDE AND DIRECTION OF VELOCITY CHANGE FOR 300 N. MILE CIRCULAR ORBIT

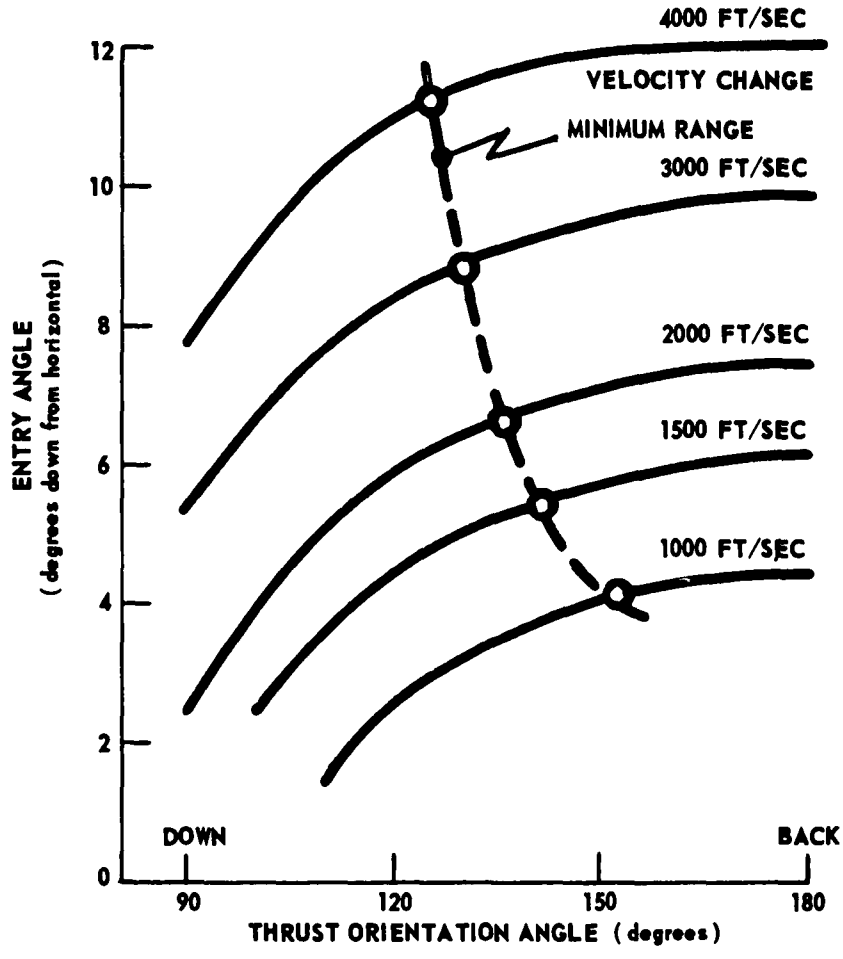

Fig. 5 ATMOSPHERIC ENTRY ANGLE VERSUS MAGNITUDE AND DIRECTION OF VELOCITY CHANGE FOR 300 N. MILE CIRCULAR ORBIT (ENTRY AT 400,000 FEET ALTITUDE)

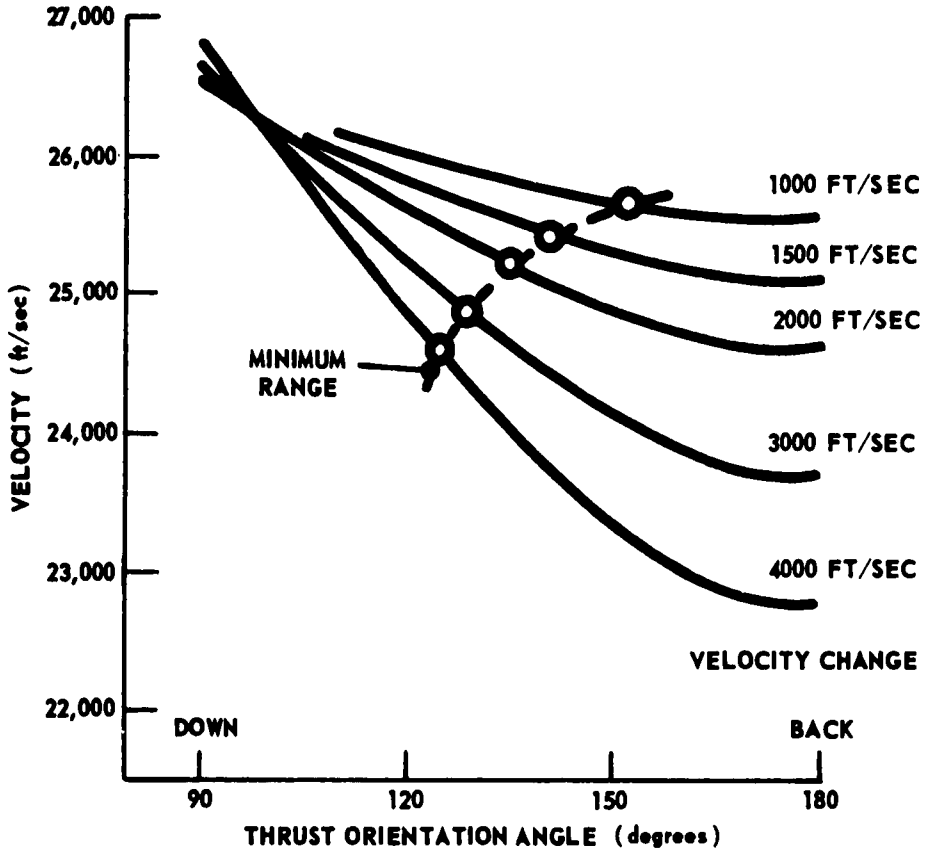

Fig. 6 ATMOSPHERIC ENTRY VELOCITY VERSUS MAGNITUDE AND DIRECTION OF VELOCITY CHANGE FOR 300 N. MILE CIRCULAR ORBIT (ENTRY AT 400,000 FEET ALTITUDE)

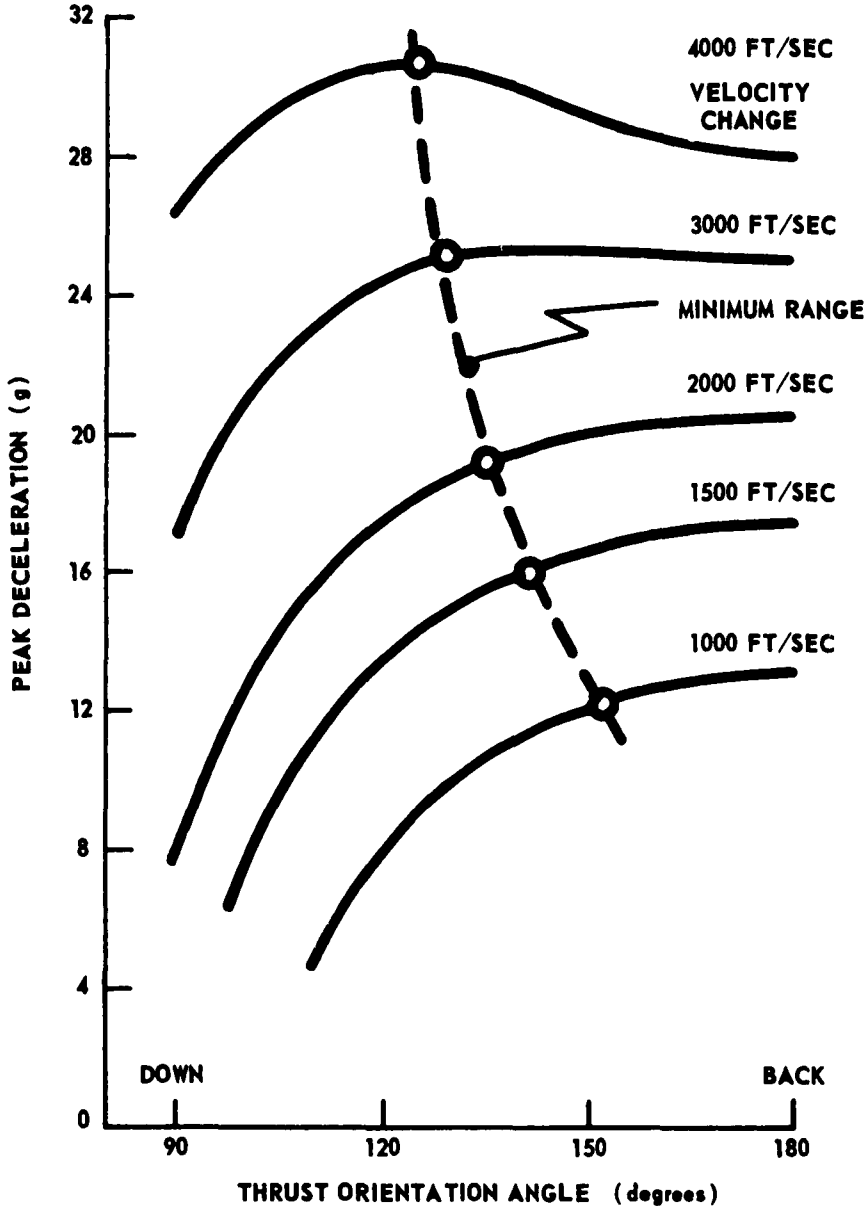

Fig. 7 PEAK DECELERATION VERSUS MAGNITUDE AND DIRECTION OF VELOCITY CHANGE FOR 300 N. MILE CIRCULAR ORBIT

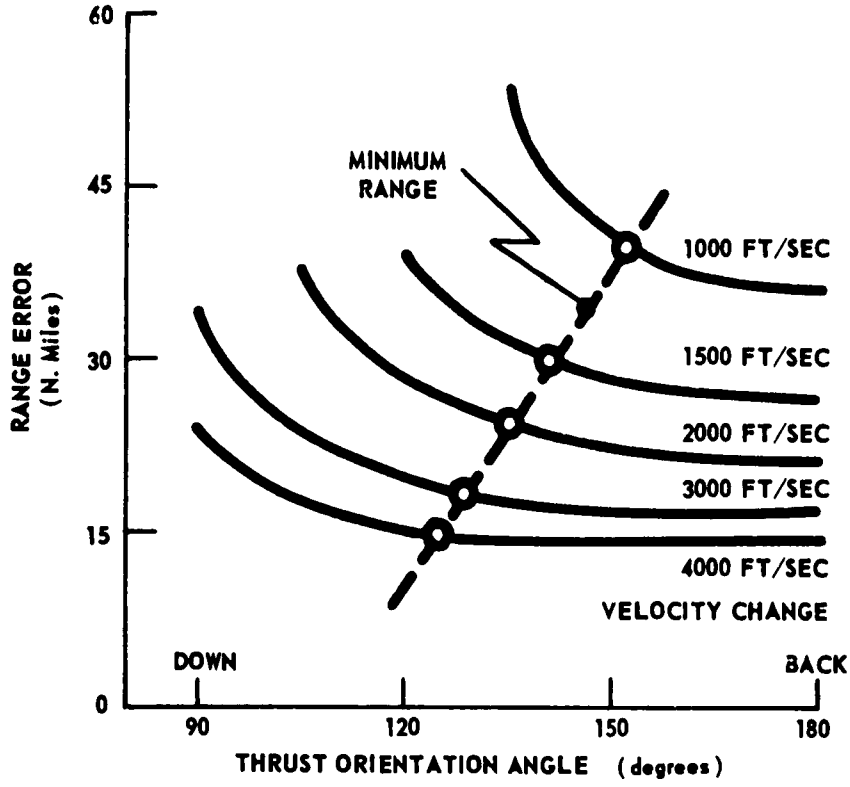

Fig. 8 RANGE ERROR PER PER CENT VARIATION IN VELOCITY CHANGE VERSUS MAGNITUDE AND DIRECTION OF VELOCITY CHANGE

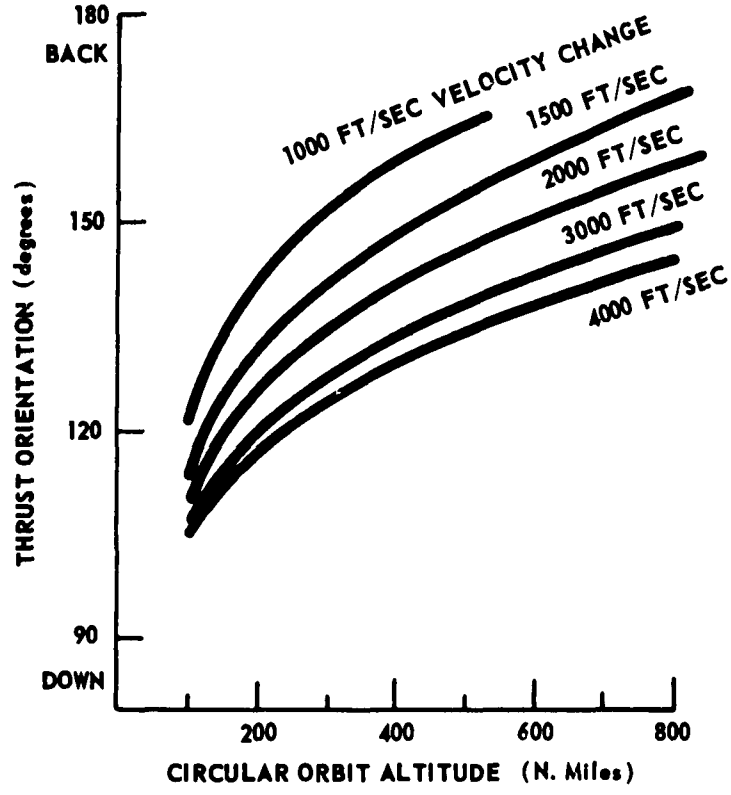

Fig. 9 THRUST ORIENTATION ANGLE FOR MINIMUM RANGE VERSUS CIRCULAR ORBIT ALTITUDE

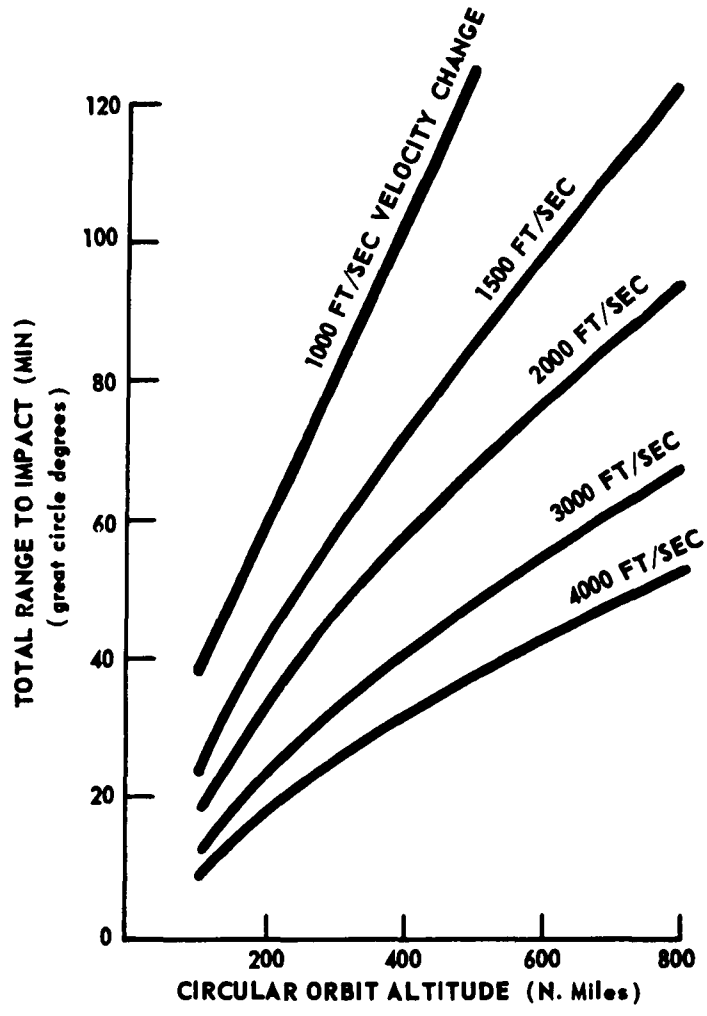

Fig. 10 MINIMUM RANGE TO IMPACT VERSUS CIRCULAR ORBIT ALTITUDE

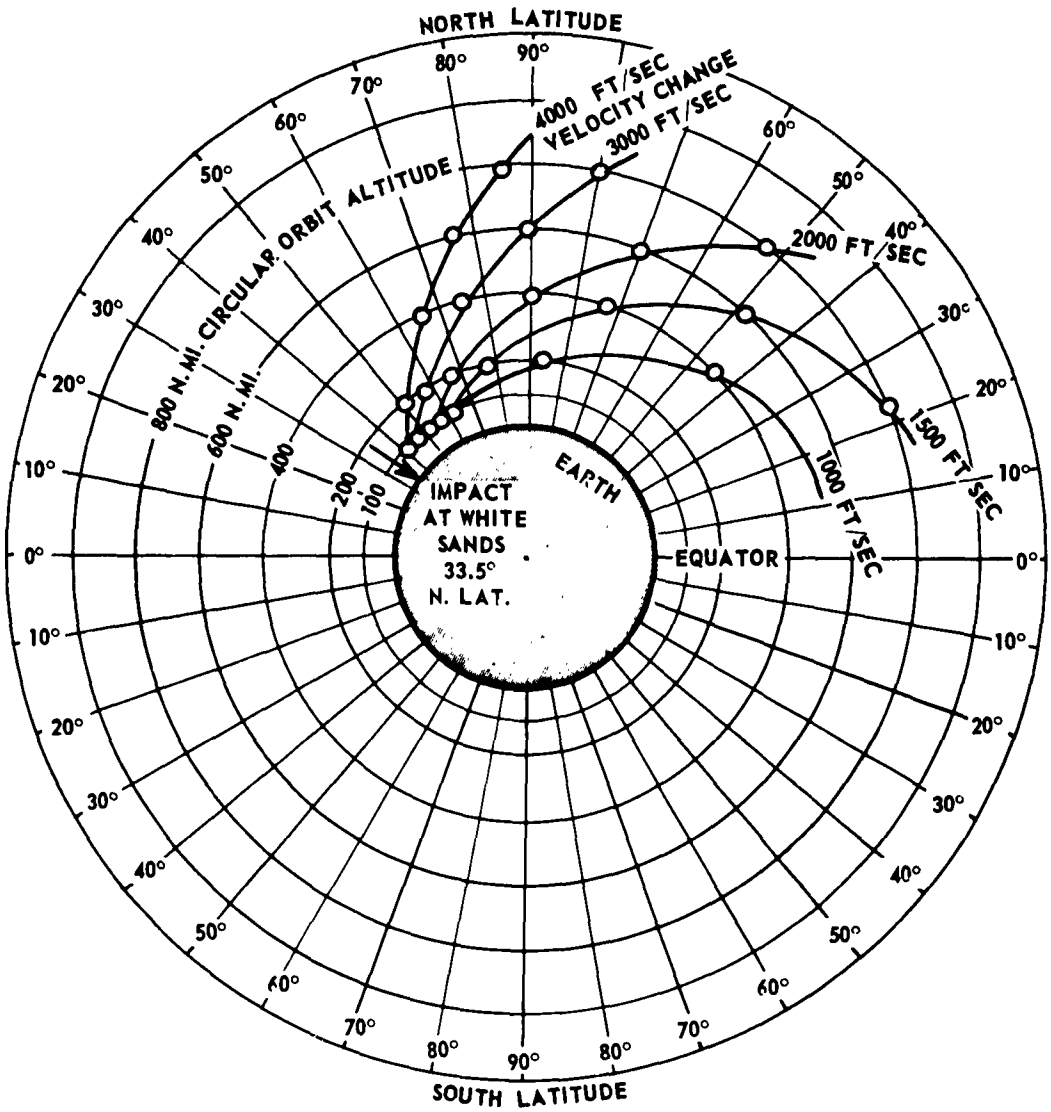

Fig. 11 ORBIT DEFLECTION LATITUDE FOR MINIMUM RANGE TO IMPACT AT WHITE SANDS (DESCENDING PASS)

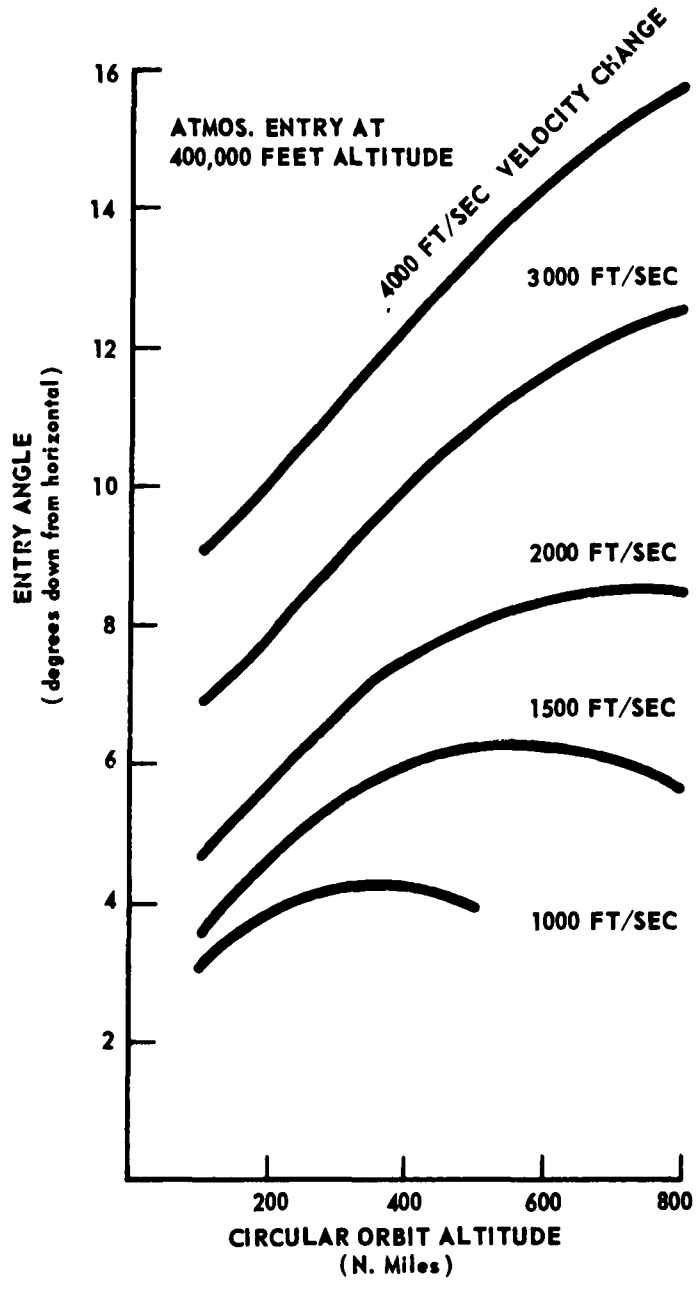

Fig. 12 ATMOSPHERIC ENTRY ANGLE FOR MINIMUM RANGE TO IMPACT VERSUS CIRCULAR ORBIT ALTITUDE (ENTRY AT 400,000 FEET ALTITUDE)

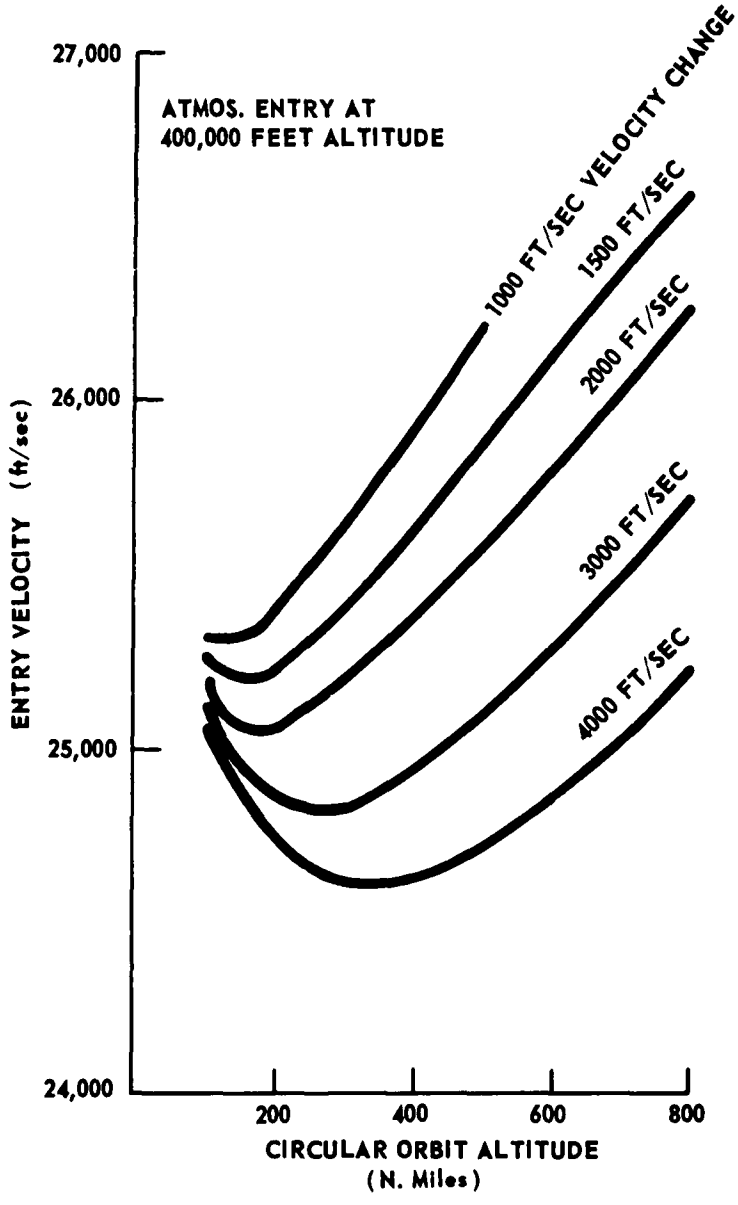

Fig. 13 ATMOSPHERIC ENTRY VELOCITY FOR MINIMUM RANGE TO IMPACT VERSUS CIRCULAR ORBIT ALTITUDE (ATMOSPHERIC ENTRY AT 400,000 FEET ALTITUDE)

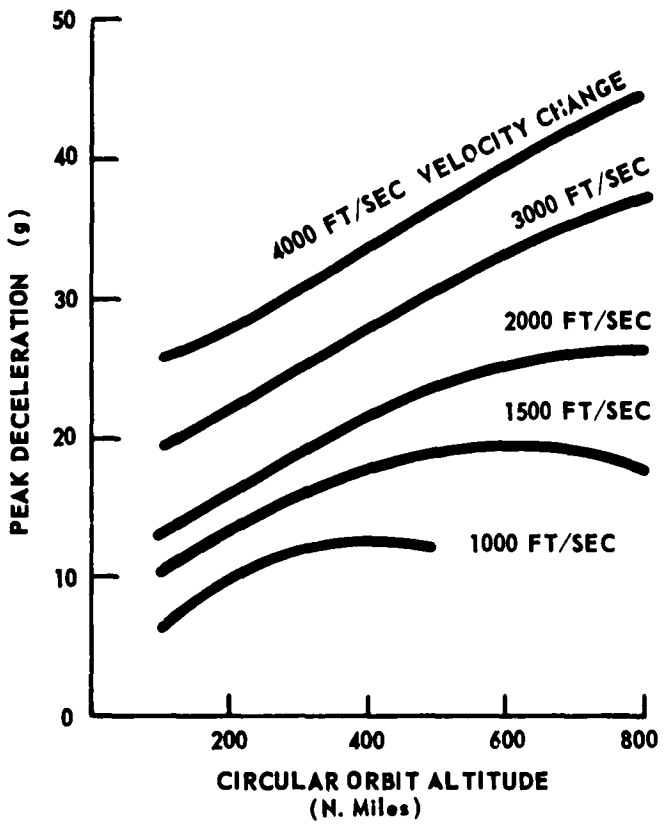

Fig. 14 PEAK DECELERATION FOR MINIMUM RANGE TO IMPACT VERSUS CIRCULAR ORBIT ALTITUDE

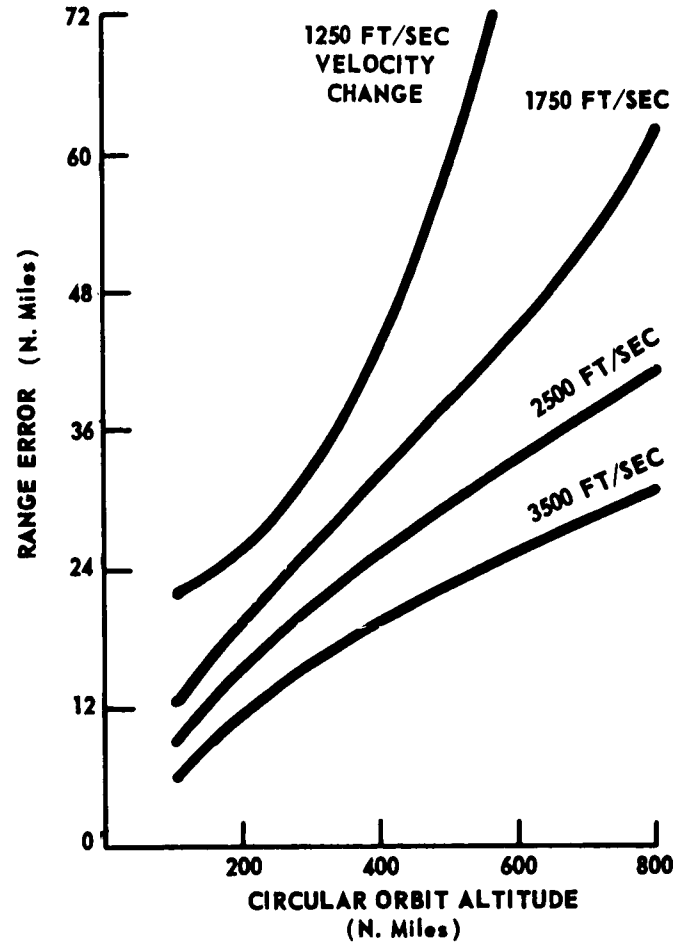

Fig. 15 RANGE ERROR PER PER CENT VARIATION IN VELOCITY CHANGE FOR MINIMUM RANGE TO IMPACT VERSUS CIRCULAR ORBIT ALTITUDE

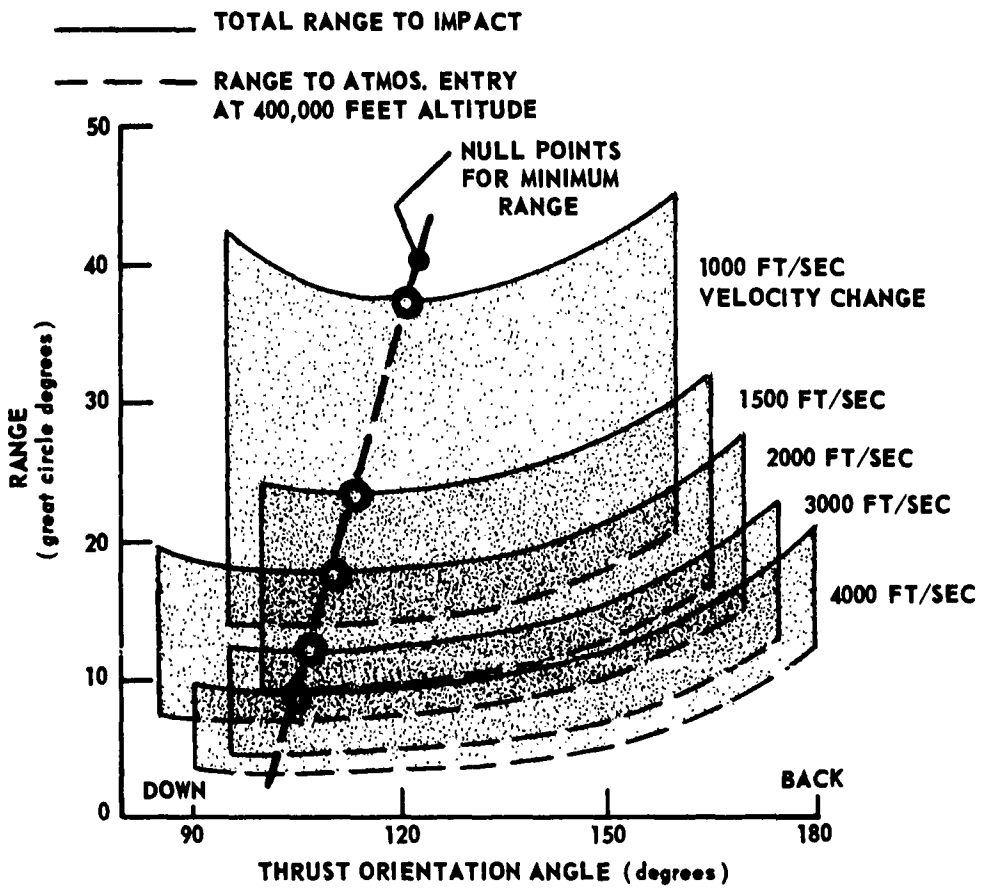

Fig. 16 RANGE VERSUS MAGNITUDE AND DIRECTION OF VELOCITY CHANGE FOR 100 N. MILE CIRCULAR ORBIT

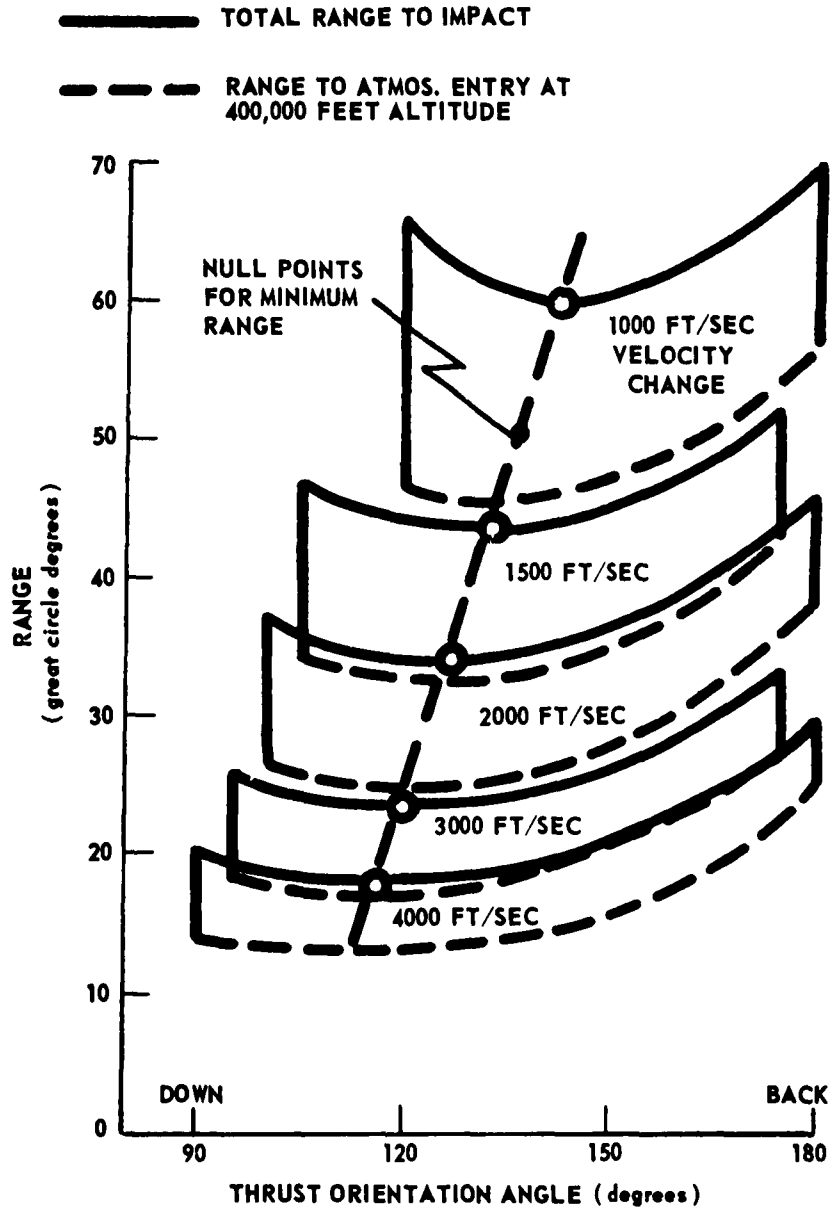

Fig. 17 RANGE VERSUS MAGNITUDE AND DIRECTION OF VELOCITY CHANGE FOR 200 N. MILE CIRCULAR ORBIT

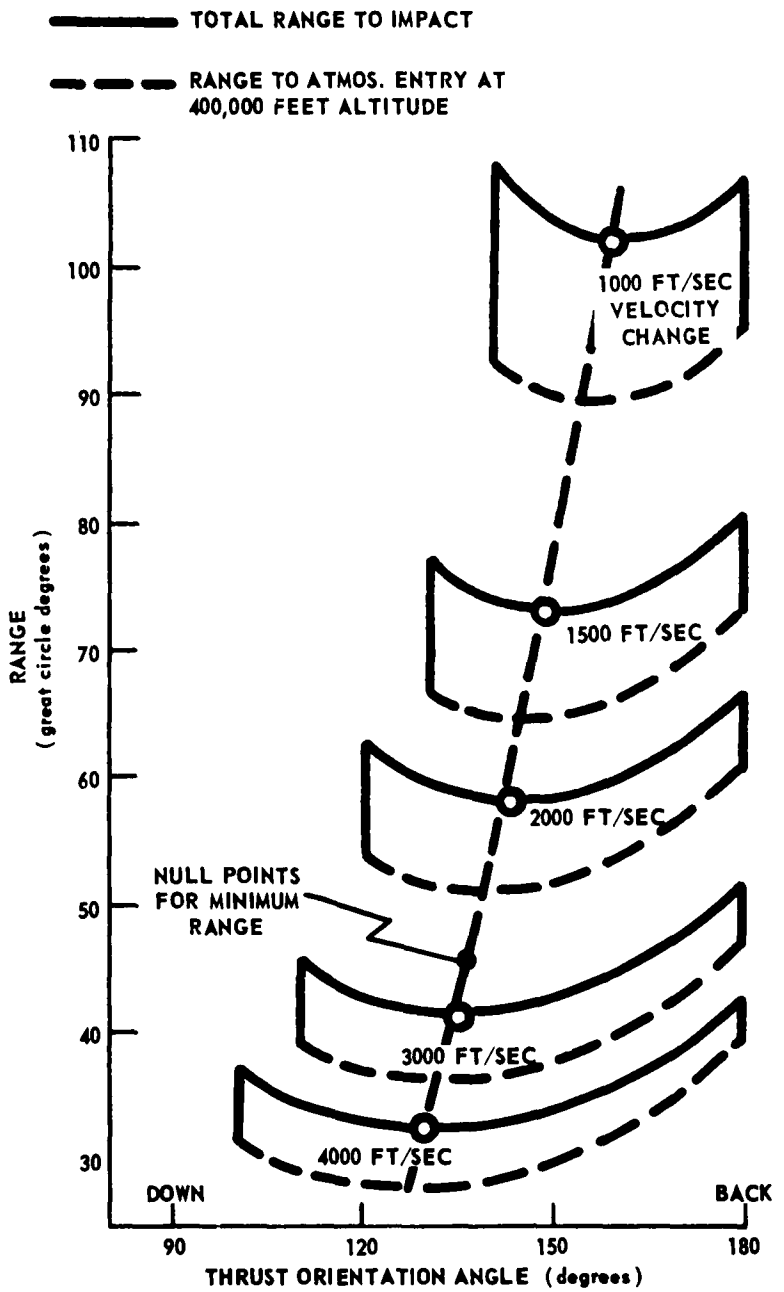

Fig. 18 RANGE VERSUS MAGNITUDE AND DIRECTION OF VELOCITY CHANGE FOR 400 N. MILE CIRCULAR ORBIT

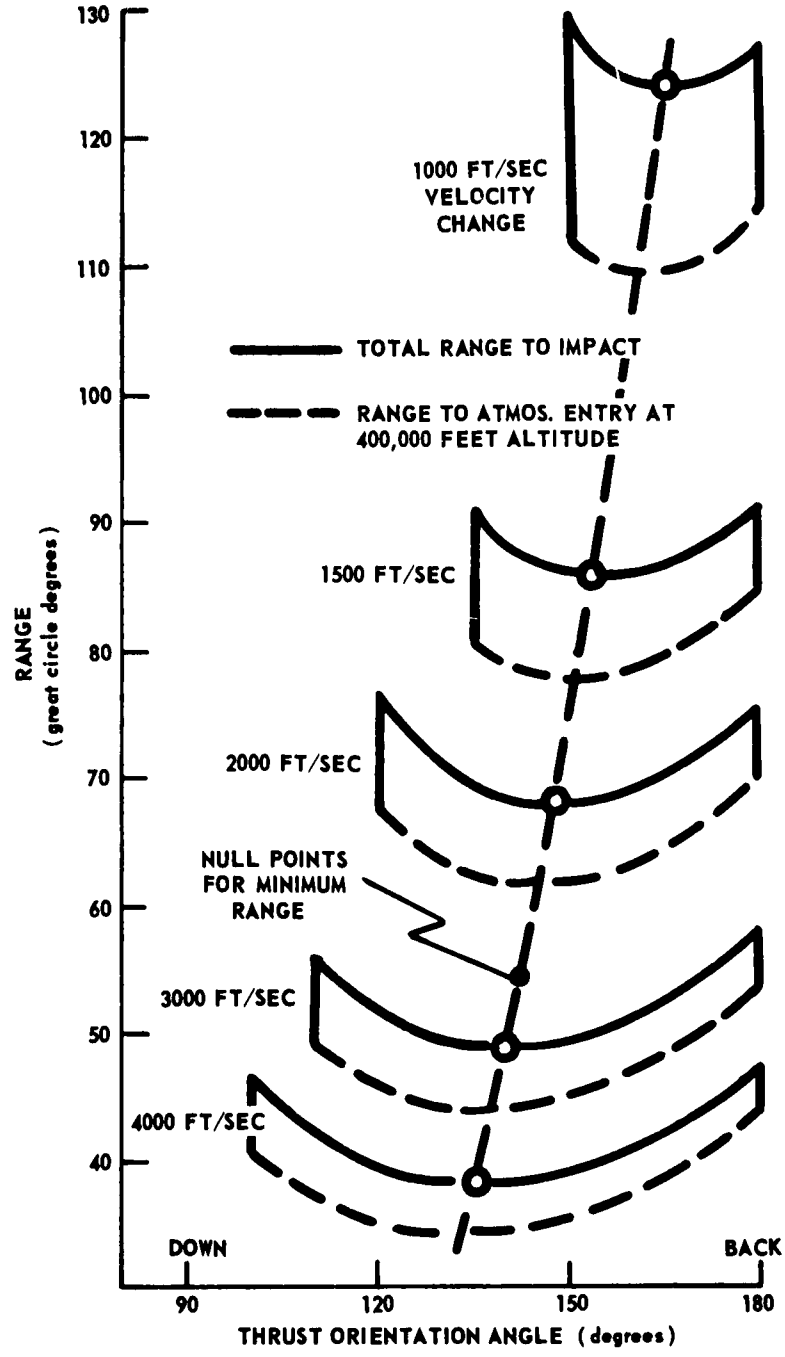

Fig. 10 RANGE VERSUS MAGNITUDE AND DIRECTION OF VELOCITY CHANGE FOR 500 N. MILE CIRCULAR ORBIT

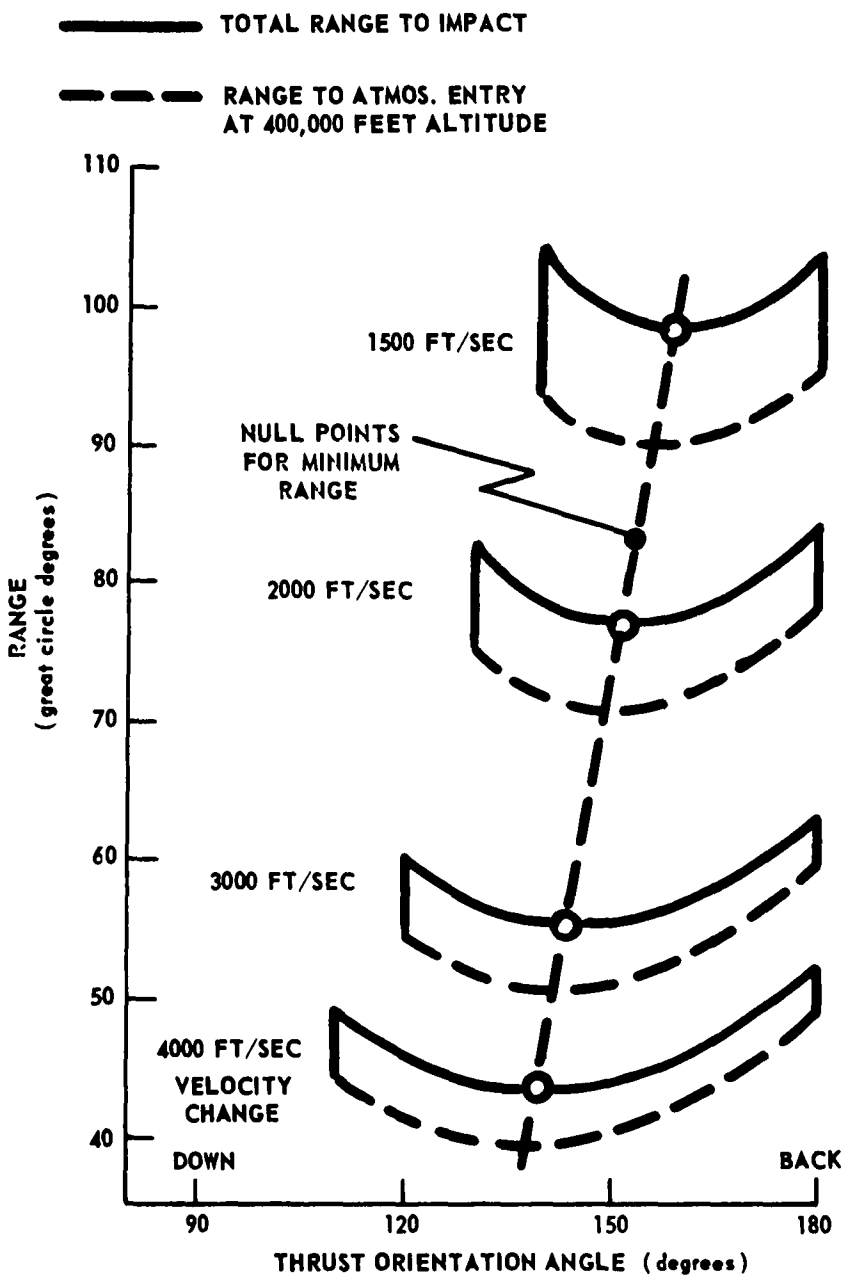

Fig. 20 RANGE VERSUS MAGNITUDE AND DIRECTION OF VELOCITY CHANGE FOR 600 N. MILE CIRCULAR ORBIT

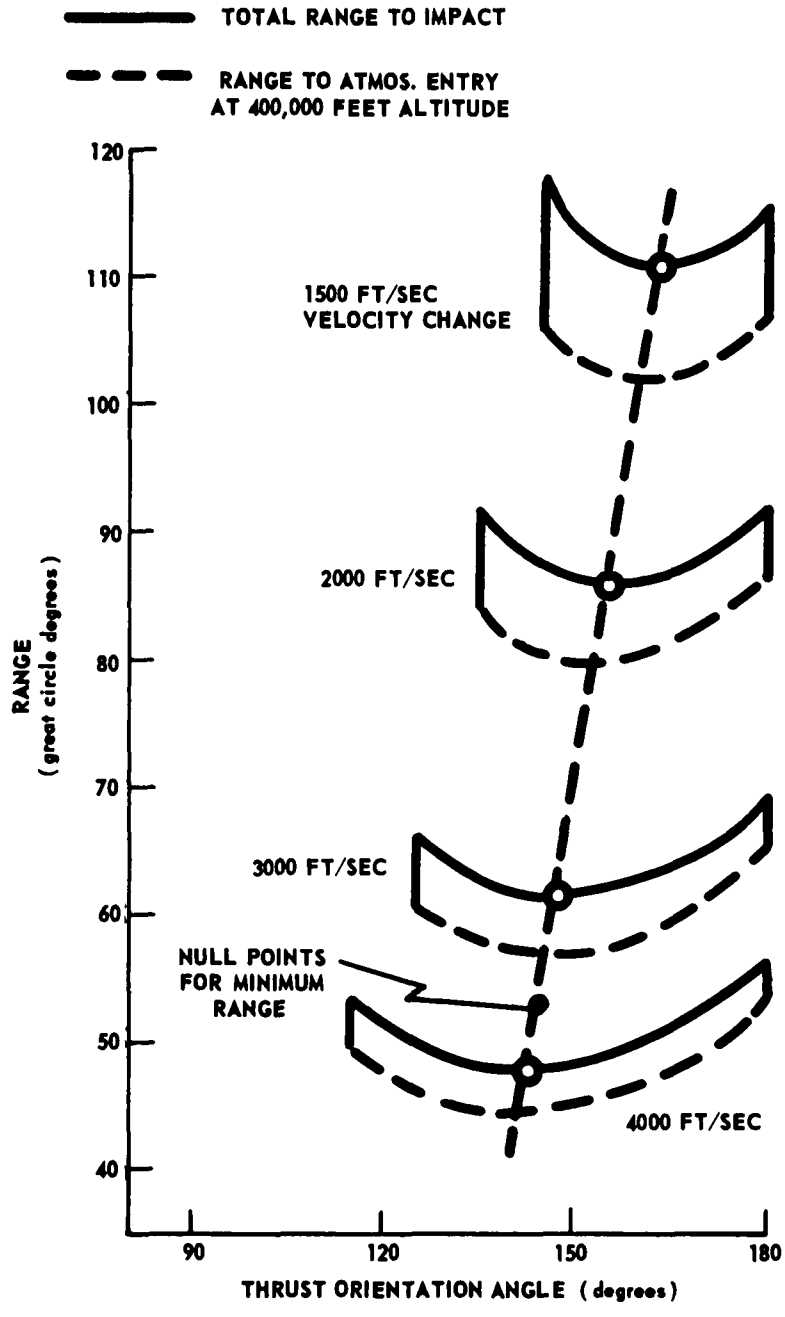

Fig. 21 RANGE VERSUS MAGNITUDE AND DIRECTION OF VELOCITY CHANGE FOR 700 N. MILE CIRCULAR ORBIT

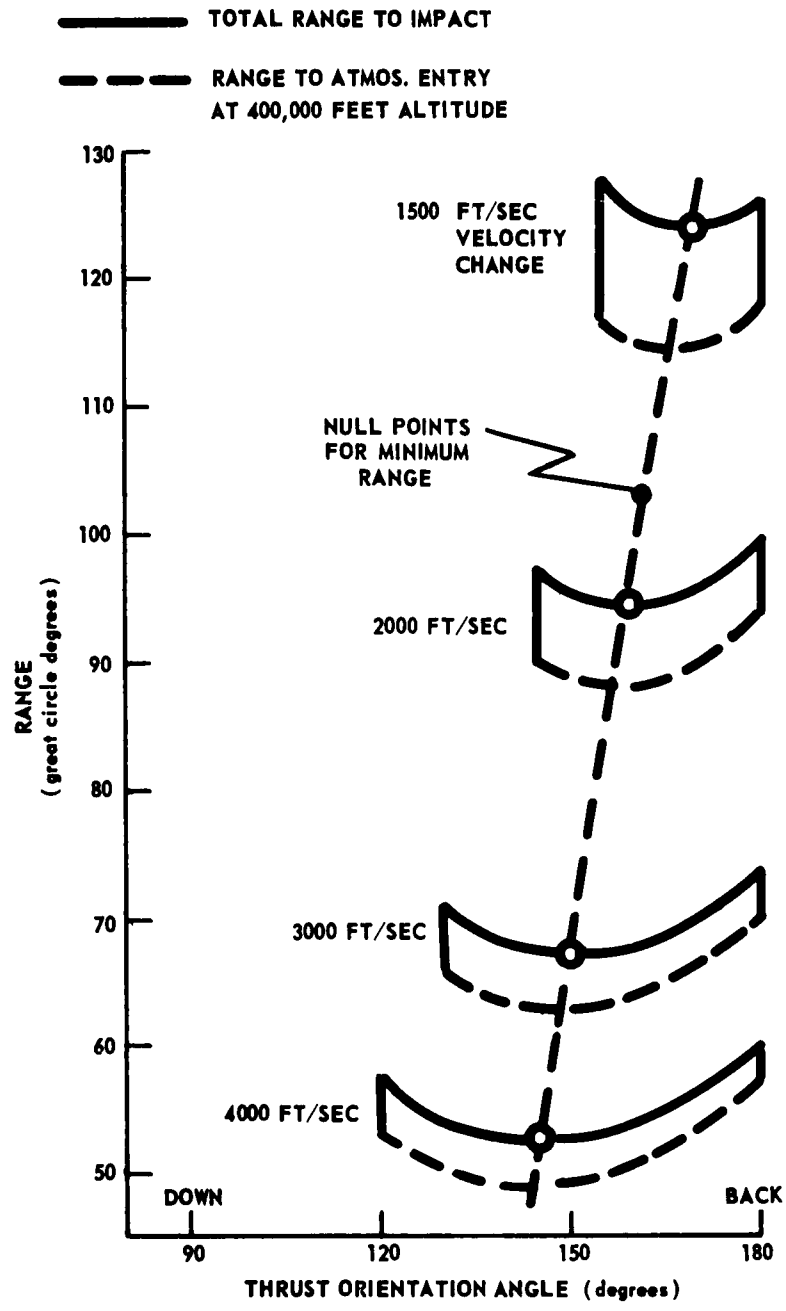

Fig. 22 RANGE VERSUS MAGNITUDE AND DIRECTION OF VELOCITY CHANGE FOR 800 N. MILE CIRCULAR ORBIT

Table I

Descent from Circular Orbit, Altitude 100 N. Miles

Thrust Orientation (degrees)		90° (down)	105°	120°	135°	150°	165°	180° (back)
Velocity Change (ft sec)	1000							
Peak Deceleration (g)			7.06	7.16	6.958	6.615	6.307	6.184
Entry Angle (degrees)			2.38	2.46	2.43	2.34	2.25	2.21
Entry Velocity (ft sec)			25577	25334	25124	24962	24860	24825
Vacuum Range (degrees)			13.86	14.24	15.548	17.983	21.948	28.018
Atmospheric Range (degrees)			25.0	23.3	21.7	24.2	24.2	24.2
Total Range (degrees)			38.9	37.5	37.2	42.2	46.2	52.2
Velocity Change (ft sec)	1500							
Peak Deceleration (g)		9.94	10.30	10.03	9.34	8.48	7.75	7.47
Entry Angle (degrees)		3.28	3.50	3.51	3.35	3.11	2.88	2.78
Entry Velocity (ft sec)		25858	25471	25106	24787	24540	24384	24330
Vacuum Range (degrees)		9.55	9.33	9.74	10.86	12.96	16.58	22.44
Atmospheric Range (degrees)		16.70	14.3	13.9	13.8	14.3	15.3	15.9
Total Range (degrees)		26.30	23.6	23.6	24.7	27.3	31.9	38.3
Velocity Change (ft sec)	2000							
Peak Deceleration (g)		13.35	13.49	12.80	11.569	10.131	8.930	8.449
Entry Angle (degrees)		4.40	4.62	4.56	4.27	3.84	3.45	3.28
Entry Velocity (ft sec)		25892	25376	24885	24456	24121	23908	23835
Vacuum Range (degrees)		7.13	7.03	7.42	8.405	10.302	13.718	19.582
Atmospheric Range (degrees)		11.8	10.8	10.5	10.8	11.3	12.5	12.7
Total Range (degrees)		18.95	17.82	17.87	19.116	21.437	25.926	31.795
Velocity Change (ft sec	3000							
Peak Deceleration (g)		20.19	19.77	18.15	15.741	13.060	10.799	9.869
Entry Angle (degrees)		6.61	6.87	6.70	6.13	5.31	4.52	4.17
Entry Velocity (ft sec)		25988	25213	24468	23810	23293	22961	22847
Vacuum Range (degrees)		4.76	4.67	4.92	5.602	6.997	9.754	15.057
Atmospheric Range (degrees)		7.8	7.3	7.3	7.8	8.7	9.5	10.0
Total Range (degrees)		12.56	11.97	12.22	13.402	15.697	19.254	25.057
Velocity Change (ft/sec)	4000							
Peak Deceleration (g)		27.10	25.98	23.30	19.630	15.640	12.250	10.818
Entry Angle (degrees)		8.79	9.14	8.89	8.08	6.84	5.58	5.00
Entry Velocity (ft/sec)		26123	25089	24086	23190	24478	22019	21860
Vacuum Range (degrees)		3.57	3.49	3.66	4.166	5.268	7.612	12.583
Atmospheric Range (degrees)		5.9	5.6	5.6	6.0	6.8	7.9	8.3
Total Range (degrees)		9.47	9.09	9.26	10.166	12.068	15.512	20.883

Table II

Descent from Circular Orbit, Altitude 200 N. Miles

Thrust Orientation (degrees)		90° (down)	105°	120°	135°	150°	165°	180° (back)
Velocity Change (ft sec)	1000							
Peak Deceleration (g)		1.81	6.79	8.87	10.07	10.75	11.09	11.19
Entry Angle (degrees)		0.58	2.23	2.96	3.42	3.70	3.84	3.89
Entry Velocity (ft sec)		26179	25928	25693	25489	25331	25231	25197
Vacuum Range (degrees)		74.55	51.59	46.58	45.63	47.16	50.85	56.87
Atmospheric Range (degrees)				20.0	15.0	13.3	12.8	12.5
Total Range (degrees)				66.6	60.6	60.4	63.3	69.4
Velocity Change (ft sec)	1500							
Peak Deceleration (g)		7.83	11.00	12.67	13.52	13.90	14.03	14.06
Entry Angle (Degrees)		2.51	3.64	4.31	4.71	4.94	5.05	5.08
Entry Velocity (ft sec)		26203	25826	25471	25161	24921	24769	24717
Vacuum Range (degrees)		39.98	34.18	32.46	32.89	35.04	38.97	45.00
Atmospheric Range (degrees)		30.0	12.7	11.7	10.5	9.9	9.6	9.4
Total Range (degrees)		70.0	46.9	44.2	43.4	44.9	48.6	54.4
Velocity Change (ft sec)	2000							
Peak Deceleration (g)		11.95	14.68	15.97	16.42	16.41	16.28	16.20
Entry Angle (degrees)		3.83	4.89	5.53	5.88	6.04	6.08	6.09
Entry Velocity (ft sec)		26236	25734	25257	24840	24515	24309	24238
Vacuum Range (degrees)		28.81	25.77	25.06	25.89	28.17	32.09	38.07
Atmospheric Range (degrees)		14.7	10.3	9.2	8.3	8.1	8.0	8.0
Total Range (degrees)		43.51	36.07	34.26	34.19	36.27	40.09	46.07
Velocity Change (ft sec)	3000							
Peak Deceleration (g)		19.44	21.51	21.94	21.39	20.44	19.61	19.28
Entry Angle (degrees)		6.19	7.27	7.86	8.07	8.04	7.93	7.87
Entry Velocity (ft/sec)		26331	25577	24853	24215	23713	23392	23282
Vacuum Range (degrees)		18.74	17.32	17.20	18.17	20.35	24.07	29.84
Atmospheric Range (degrees)		8.5	7.0	6.3	6.2	6.0	6.0	6.0
Total Range (degrees)		27.24	24.32	23.50	24.37	26.35	30.07	35.84
Velocity Change (ft/sec)	4000							
Peak Deceleration (g)		26.70	28.06	27.45	25.72	23.64	21.99	21.35
Entry Angle (degrees)		8.44	9.59	10.15	10.22	9.97	9.63	9.49
Entry Velocity (ft/sec)		26464	25458	24484	23616	22927	22483	22330
Vacuum Range (degrees)		13.94	13.01	13.02	13.90	15.86	19.31	24.86
Atmospheric Range (degrees)		6.2	5.3	5.1	5.0	5.0	5.1	5.2
Total Range (degrees)		20.14	18.31	18.12	18.90	20.86	24.41	30.06

Table III

Descent from Circular Orbit, Altitude 300 N. Miles

Thrust Orientation (degrees		90° (down)	105°	120°	135°	150°	165°	180° (back)
Velocity Change (ft sec)	1000							
Peak Deceleration (g)				7.98	10.67	12.18	12.98	13.22
Entry Angle (degrees)				2.60	3.53	4.08	4.38	4.47
Entry Velocity (ft sec)				26028	25829	25674	25578	25545
Vacuum Range (degrees)				76.97	70.14	69.12	71.62	77.30
Atmospheric Range (degrees)				26.7	15.7	12.5	11.7	11.2
Total Range (degrees)				103.67	85.84	81.62	83.32	88.50
Velocity Change (ft sec)	15000							
Peak Deceleration (g)			9.58	13.42	15.54	16.73	17.33	17.52
Entry Angle (degrees)			3.09	4.44	5.27	5.78	6.06	6.15
Entry Velocity (ft sec)			26158	25812	25511	25277	25129	25079
Vacuum Range (degrees)			59.50	52.01	50.04	51.01	54.38	60.24
Atmospheric Range (degrees)			20.0	11.7	9.7	8.9	8.0	7.8
Total Range (degrees)			80.0	63.7	59.7	59.9	62.4	68.0
Velocity Change (ft sec)	2000							
Peak Deceleration (g)		7.703	14.357	17.563	19.282	20.153	20.536	20.641
Entry Angle (degrees)		2.41	4.66	5.92	6.71	7.20	7.45	7.53
Entry Velocity (ft sec)		26558	26068	25604	25198	24883	24682	24613
Vacuum Range (degrees)		56.079	43.715	40.040	39.506	41.119	44.739	50.622
Atmospheric Range (degrees)		33.3	11.3	8.6	7.5	7.0	6.7	6.5
Total Range (degrees)		89.379	55.015	48.640	47.006	48.119	51.439	57.122
Velocity Change (ft sec)	3000							
Peak Deceleration (g)		17.309	22.221	24.494	25.304	25.358	25.169	25.067
Entry Angle (degrees)		5.38	7.31	8.53	9.27	9.67	9.85	9.90
Entry Velocity (ft sec)		26652	25917	25213	24592	24105	23794	23687
Vacuum Range (degrees)		33.587	29.089	27.654	28.035	29.993	33.663	39.433
Atmospheric Range (degrees)		10.2	7.0	5.9	5.4	5.3	5.1	5.1
Total Range (degrees)		43.787	36.089	33.554	33.435	35.293	38.763	44.533
Velocity Change (ft sec)	4000							
Peak Deceleration (g)		25.330	29.327	30.580	30.279	29.317	28.411	28.050
Entry Angle (degrees)		7.81	9.76	10.98	11.66	11.95	12.02	12.02
Entry Velocity (ft sec)		26783	25803	24856	24013	23345	22915	22767
Vacuum Range (degrees)		24.513	21.858	21.090	21.682	23.617	27.146	32.740
Atmospheric Range (degrees)		6.9	5.3	4.8	4.4	4.3	4.3	4.3
Total Range (degrees)		31.413	27.158	25.890	26.082	27.917	31.446	37.040

Table IV

Descent from Circular Orbit, Altitude 400 N. Miles

Thrust Orientation (degrees)		90° (down)	105°	120°	135°	150°	165°	180° (back)
Velocity Change (ft sec)	1000							
Peak Deceleration (g)					9.274	11.932	13.257	13.666
Entry Angle (degrees)					2.99	3.90	4.36	4.51
Entry Velocity (ft sec)					26148	25998	25903	25871
Vacuum Range (degrees)					95.22	89.71	90.44	95.61
Atmospheric Range (degrees)					20.0	13.7	12.2	11.5
Total Range (degrees)					115.2	103.4	102.6	107.1
Velocity Change (ft sec)	1500							
Peak Deceleration (g)				12.63	16.21	18.21	19.25	19.57
Entry Angle (degrees)				4.08	5.36	6.13	6.56	6.69
Entry Velocity (ft sec)				26131	25838	25610	25466	25417
Vacuum Range (degrees)				71.31	65.54	64.83	67.42	73.05
Atmospheric Range (degrees)				13.1	9.7	8.3	7.8	7.5
Total Range (degrees)				84.4	75.2	73.1	75.2	80.6
Velocity Change (ft sec)	2000							
Peak Deceleration (g)			12.43	17.99	20.97	22.62	23.44	23.68
Entry Angle (degrees)			3.94	5.91	7.11	7.86	8.28	8.41
Entry Velocity (ft sec)			26382	25929	25534	25226	25031	24964
Vacuum Range (degrees)			62.85	53.98	51.42	52.04	55.18	60.92
Atmospheric Range (degrees)			12.5	8.8	7.2	6.3	6.0	6.0
Total Range (degrees)			75.35	62.78	58.62	58.34	61.18	66.92
Velocity Change (ft sec)	3000							
Peak Deceleration (g)		13.17	22.01	26.16	28.19	29.06	29.36	29.42
Entry Angle (degrees)		4.00	7.07	8.87	10.04	10.76	11.15	11.27
Entry Velocity (ft sec)		26952	26235	25549	24945	24471	24169	24069
Vacuum Range (degrees)		51.18	40.56	37.11	36.52	38.00	41.43	47.13
Atmospheric Range (degrees)		15.0	7.3	5.8	5.1	4.8	4.7	4.6
Total Range (degrees)		66.18	47.86	42.91	41.63	42.80	46.13	51.73
Velocity Change (ft sec)	4000							
Peak Deceleration (g)		22.84	29.90	32.96	33.91	33.82	33.45	33.27
Entry Angle (degrees)		6.88	9.70	11.52	12.68	13.36	13.69	13.79
Entry Velocity (ft sec)		27082	26126	25203	24383	23735	23318	23174
Vacuum Range (degrees)		35.76	30.31	28.36	28.38	30.03	33.44	39.00
Atmospheric Range (degrees)		7.8	5.3	4.6	4.2	3.9	3.8	3.75
Total Range (degrees)		43.56	35.61	32.96	32.58	33.93	37.24	42.75

Table V

Descent from Circular Orbit, Altitude 500 N. Miles

Thrust Orientation (degrees)		90° (down)	105°	120°	135°	150°	165°	180° (back)
Velocity Change (ft/sec)	1000							
Peak Deceleration (g)					4.26	9.89	12.07	12.70
Entry Angle (degrees)					1.34	3.15	3.87	4.09
Entry Velocity (ft/sec)					26446	26300	26208	26177
Vacuum Range (degrees)					131.97	112.09	109.64	114.01
Atmospheric Range (degrees)						18.3	14.2	13.0
Total Range (degrees)						130.4	123.8	127.0
Velocity Change (ft/sec)	1500							
Peak Deceleration (g)				9.96	15.71	18.66	20.17	20.64
Entry Angle (degrees)				3.14	5.07	6.13	6.70	6.89
Entry Velocity (ft/sec)				26431	26144	25922	25787	25734
Vacuum Range (degrees)				93.17	80.72	77.74	79.35	84.70
Atmospheric Range (degrees)				~20.0	10.5	8.3	7.5	6.5
Total Range (degrees)				~113.0	91.2	86.0	86.9	91.2
Velocity Change (ft/sec)	2000							
Peak Deceleration (g)			7.80	17.36	21.76	24.19	25.44	25.82
Entry Angle (degrees)			2.42	5.57	7.20	8.20	8.76	8.93
Entry Velocity (ft/sec)			26676	26234	25848	25549	25358	25293
Vacuum Range (degrees)			87.65	67.79	62.48	61.88	64.44	70.01
Atmospheric Range (degrees)			33.3	9.5	7.0	6.2	5.8	5.7
Total Range (degrees)			120.96	77.29	69.48	68.08	70.24	75.71
Velocity Change (ft/sec)	3000							
Peak Deceleration (g)			20.84	27.11	30.34	31.97	32.68	32.88
Entry Angle (degrees)			6.54	8.97	10.53	11.52	12.07	12.25
Entry Velocity (ft/sec)			26534	25865	25276	24814	24520	24419
Vacuum Range (degrees)			52.22	45.96	44.18	45.03	48.17	53.77
Atmospheric Range (degrees)			8.2	5.7	4.9	4.5	4.3	4.25
Total Range (degrees)			60.4	51.7	49.1	49.5	52.5	58.0
Velocity Change (ft/sec)	4000							
Peak Deceleration (g)		18.83	29.81	34.75	36.88	37.56	37.64	37.61
Entry Angle (degrees)		5.55	9.45	11.84	13.42	14.41	14.95	15.12
Entry Velocity (ft/sec)		27312	26429	25529	24730	24099	23694	23554
Vacuum Range (degrees)		48.55	38.56	35.09	34.36	35.62	38.84	44.34
Atmospheric Range (degrees)		10.3	5.6	4.4	3.9	3.7	3.6	3.5
Total Range (degrees)		58.9	44.2	39.5	38.3	39.3	42.4	47.8

Table VI

Descent from Circular Orbit, Altitude 600 N. Miles

Thrust Orientation (degrees)		90° (down)	105°	120°	135°	150°	165°	180° (back)
Velocity Change (ft/sec)	1000							
Peak Deceleration (g)							8.81	9.93
Entry Angle (degrees)							2.77	3.13
Entry Velocity (ft/sec)							26495	26464
Vacuum Range (degrees)							132.49	135.07
Atmospheric Range (degrees							28.3	21.7
Total Range (degrees)							160.8	156.8
Velocity Change (ft/sec)	1500							
Peak Deceleration (g)					13.94	18.16	20.23	20.86
Entry Angle (degrees)					4.40	5.84	6.57	6.80
Entry Velocity (ft/sec)					26433	26216	26079	26032
Vacuum Range (degrees)					96.12	90.48	90.82	95.81
Atmospheric Range (degrees)					12.5	9.0	7.9	7.6
Total Range (degrees)					108.6	99.5	98.7	103.4
Velocity Change (ft/sec)	2000							
Peak Deceleration (g)				15.54	21.75	25.05	26.73	27.25
Entry Angle (degrees)				4.88	7.03	8.29	8.98	9.21
Entry Velocity (ft/sec)				26521	26144	25852	25666	25602
Vacuum Range (degrees)				82.41	73.19	71.09	72.99	78.36
Atmospheric Range (degrees)				11.0	7.3	6.2	5.7	5.6
Total Range (degrees)				93.41	80.49	77.29	78.69	83.96
Velocity Change (ft/sec)	3000							
Peak Deceleration (g)			18.57	27.42	31.90	34.26	35.38	35.71
Entry Angle (degrees)			5.70	8.87	10.81	12.04	12.74	12.96
Entry Velocity (ft/sec)			26815	26161	25587	25137	24850	24751
Vacuum Range (degrees)			64.71	54.49	51.26	51.42	54.21	59.70
Atmospheric Range (degrees)			9.8	5.8	4.8	4.3	4.2	4.1
Total Range (degrees)			74.5	60.3	56.1	55.7	58.4	63.8
Velocity Change (ft/sec)	4000							
Peak Deceleration (g)		11.86	29.08	36.02	39.32	40.73	41.21	41.31
Entry Angle (degrees)		3.43	9.02	11.98	13.94	15.21	15.92	16.14
Entry Velocity (ft/sec)		27626	26714	25836	25056	24416	24047	23911
Vacuum Range (degrees)		65.60	46.81	41.42	39.83	40.64	43.64	49.05
Atmospheric Range (degrees)		21.7	5.8	4.4	3.8	3.5	3.3	3.3
Total Range (degrees)		87.3	52.6	45.8	43.6	44.1	46.9	52.3

Table VII

Descent from Circular Orbit, Altitude 700 N. Miles

Thrust Orientation (degrees)		90° (down)	105°	120°	135°	150°	165°	180° (back)
Velocity Change (ft/sec)	1000							
Peak Deceleration (g)								
Entry Angle (degrees								
Entry Velocity (ft/sec)								
Vacuum Range (degrees)								
Atmospheric Range (degrees)								
Total Range (degrees)								
Velocity Change (ft/sec)	1500							
Peak Deceleration (g)					10.28	16.65	19.46	20.30
Entry Angle (degrees)					3.18	5.24	6.19	6.48
Entry Velocity (ft/sec)					26705	26493	26359	26313
Vacuum Range (degrees)					116.16	103.75	102.32	106.86
Atmospheric Range (degrees)					20.0	10.2	8.5	8.0
Total Range (degrees)					136.2	114.0	110.8	114.9
Velocity Change (ft/sec)	2000							
Peak Deceleration (g)				12.03	20.95	25.27	27.43	28.10
Entry Angle (degrees)				3.70	6.63	8.18	9.02	9.28
Entry Velocity (ft/sec)				26791	26423	26137	25955	25893
Vacuum Range (degrees)				99.55	83.94	79.98	81.11	86.25
Atmospheric Range (degrees)				15.8	8.0	6.3	5.8	5.5
Total Range (degrees)				115.35	91.94	86.28	86.91	91.75
Velocity Change (ft/sec)	3000							
Peak Deceleration (g)			14.72	27.10	32.95	36.06	37.58	38.03
Entry Angle (degrees)			4.43	8.58	10.91	12.38	13.21	13.47
Entry Velocity (ft/sec)			27080	26441	25879	25440	25160	25063
Vacuum Range (degrees)			79.26	62.89	57.97	57.34	59.76	65.14
Atmospheric Range (degrees)			13.0	6.2	4.8	4.3	4.0	3.9
Total Range (degrees)			92.3	69.1	62.8	61.6	63.8	69.0
Velocity Change (ft/sec)	4000							
Peak Deceleration (g)			27.65	36.83	41.317	43.44	44.31	44.54
Entry Angle (degrees)			8.40	11.99	14.31	15.82	16.67	16.95
Entry Velocity (ft/sec)			26983	26124	25363	29763	24379	24246
Vacuum Range (degrees)			55.35	47.49	44.92	45.24	47.98	53.32
Atmospheric Range (degrees)			6.3	4.4	3.8	3.3	3.2	3.2
Total Range (degrees)			60.93	51.44	48.33	48.17	50.81	56.15

Table VIII

Descent from Circular Orbit. Altitude 800 N. Miles

Thrust Orientation (degrees)		90° (down)	105°	120°	135°	150°	165°	180° (back)
Velocity Change (ft/sec)	1000							
Peak Deceleration (g)								
Entry Angle (degrees)								
Entry Velocity (ft/sec)								
Vacuum Range (degrees)								
Atmospheric Range (degrees)								
Total Range (degrees)								
Velocity Change (ft/sec)	1500							
Peak Deceleration (g)						13.82	17.75	18.87
Entry Angle (degrees)						4.26	5.53	5.90
Entry Velocity (ft/sec)						26754	26623	26578
Vacuum Range (degrees)						118.66	114.41	118.29
Atmospheric Range (degrees)						13.0	9.7	7.7
Total Range (degrees)						131.7	124.1	126.0
Velocity Change (ft/sec)	2000							
Peak Deceleration (g)					19.28	24.87	27.58	29.41
Entry Angle (degrees)					5.98	7.89	8.87	9.19
Entry Velocity (ft/sec)					26686	26406	26229	26168
Vacuum Range (degrees)					95.18	88.76	88.97	93.86
Atmospheric Range (degrees)					9.0	6.7	5.9	5.7
Total Range (degrees)					104.18	95.46	94.87	99.56
Velocity Change (ft/sec)	3000							
Peak Deceleration (g)				26.165	33.534	37.430	39.358	39.940
Entry Angle (degrees)				8.12	10.87	12.57	13.52	13.83
Entry Velocity (ft/sec)				26704	26155	25726	25452	25358
Vacuum Range (degrees)				71.366	64.407	62.924	64.943	70.198
Atmospheric Range (degrees)				6.6	4.8	4.2	3.9	3.8
Total Range (degrees)				77.966	69.207	67.124	68.843	73.998
Velocity Change (ft/sec)	4000							
Peak Deceleration (g)			25.42	37.23	42.94	45.77	47.03	47.38
Entry Angle (degrees)			7.58	11.86	14.54	16.28	17.27	17.59
Entry Velocity (ft/sec)			27237	26396	26752	25067	24692	24562
Vacuum Range (degrees)			64.13	53.38	49.72	49.51	51.99	57.24
Atmospheric Range (degrees)			7.0	4.4	3.7	3.3	3.1	3.0
Total Range (degrees)			71.13	57.78	53.42	52.81	55.09	60.24

ACKNOWLEDGMENT

Greatful acknowledgment is due to members of the BID-4 Group for manual reduction of the data used in this report.

The Johns Hopkins University
APPLIED PHYSICS LABORATORY
Silver Spring, Maryland

The technical papers and progress reports issued by APL in the CM series are characterized by extensive treatment of their subjects. Official Laboratory review of CM reports substantiates their technical validity and establishes suitability for distribution to qualified personnel outside Section T.

Initial distribution of this document has been made in accordance with a list on file in the Technical Reports Group of the Applied Physics Laboratory, The Johns Hopkins University.